LAWRENCE
LIVERMORE
NATIONAL
LABORATORY

HOT ELECTRON ENERGY DISTRIBUTIONS FROM ULTRA-INTENSE LASER SOLID INTERACTIONS

H. Chen, S. C. Wilks, W. L. Kruer, S. Moon, N. Patel, P. K. Patel, R. Shepherd, R. Snavely

December 9, 2005

Disclaimer

The headers will be insert by the Publisher
The headers will be insert by the Publisher
The headers will be insert by the Publisher

HOT ELECTRON ENERGY DISTRIBUTIONS FROM ULTRA-INTENSE LASER SOLID INTERACTIONS

Hui Chen, S. C. Wilks, W. L. Kruer, S. Moon, N. Patel, P. K. Patel, R. Shepherd and R. Snavely

Lawrence Livermore National Laboratory, Livermore, CA 94550, USA

Abstract. We present experimental data of electron energy distributions from ultra-intense ($>10^{19}$ W/cm^2) laser-solid interactions using the Rutherford Appleton Laboratory Vulcan petawatt laser. These measurements were made using a CCD-based magnetic spectrometer. We present details on the distinct effective temperatures that were obtained for a wide variety of targets as a function of laser intensity. It is found that as the intensity increases from 10^{17} W/cm^2 to 10^{19} W/cm^2, a 0.4 dependence on the laser intensity is found. Between 10^{19} W/cm^2 and 10^{20} W/cm^2, a gradual rolling off of temperature with intensity is observed.

1. INTRODUCTION.

Hot electron generation and transport from ultra-intense laser solid interactions is fundemental to the understanding of high energy density physics. One useful metric to quantify the hot electrons generated during these interactions is the hot electron energy distribution, hereafter referred to as the effective electron temperature, T_{hot}. Although it is generally agreed that, as shown in previous studies (see review by Gibbon and Forster [1]), higher laser intensity results higher electron temperature, and at ultrahigh intensities ($I\lambda^2 > 10^{18}$ Wcm$^{-2}\mu$m^2) electrons are strongly relativistic with effective temperatures that scale with the ponderomotive potential of the laser [2], the predictions of the electron temperatures are not unambiguous due to the complicated physics processes involved. In Figure 1, we plot the data presented in Gibbon and Forster [1], along with the predictions of a set of 2D PIC simulations, as well as the ponderomotive scaling [2], which is given by

$$kT_{ho\,t} \sim m_e c^2 \left[\sqrt{1 + \frac{I\lambda^2}{2.8 \times 10^{18}}} - 1 \right] \qquad (1)$$
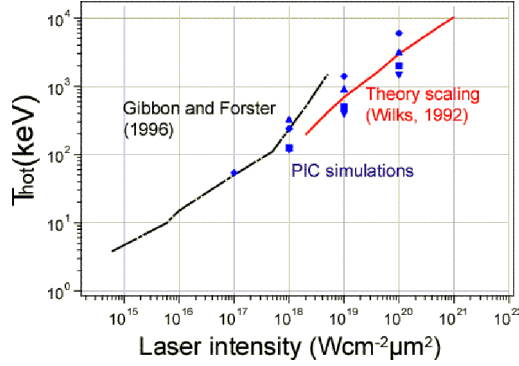
Figue 1. Hot electron temperature from simulation and theoretical scalling. The black was reproduced from the review article by Gibbon and Forster [1], which agreed well with existing experimental data. The discreate points were from our 2D PIC calculations at various conditions (from four simulation conditions: blue triangles for with prepulse at 0 degree incident angle; blue squares for no prepulse at 0 degree incident angle; blue diamonds for with prepulse at 45 degree incident angle and blue upside-down for no prepulse at 45 degree incident angle) and the red line is from theoretical scalling by Wilks et al. [2].

To measure the hot electron distribution from ultra high intense short pulse laser plasma interaction, we used a magnetic electron spectrometer that has been described previously [3]. This instrument was fielded at both the Rutherford Appleton Laboratory (RAL) Vulcan petawatt laser [4] and the LLNL Jupiter laser facility. The results from both experiments are discussed in this paper.

2. EXPERIMENTAL RESULTS

We begin by describing the experiments performed on the LLNL Jupiter facility Callisto (previously referred as JanUSP) Ti:sapphire laser. It has a pulse length of 100 fs and delivers up to 10 J laser energy at 800 nm. The laser is focused with an f/2 parabola to a focus spot size of about 3.5 μm, and the laser intensity ranges from 10^{17} - 10^{20} Wcm^{-2}. The laser is incident on the various target at 22.5 degrees off normal. The spectrometer slit is aligned 30 degrees from the laser beam, i.e. 52.5 degrees off normal, and 23 cm away from the target.

At lower intensity, we found the hot electron temperature agreed well with PIC simulations and theory [5]. At higher intensity, however, we observed hot electron temperatures approching a 'saturation' level as the laser intensity increase from mid of 10^{19} to 10^{20} Wcm^{-2}, as shown in Fig. 2. Note that the hot electron temperature is defined as the slope of the exponential decay of the distribution :

$$T_{hot} = \frac{E_1 - E_2}{\ln\left(f\left(E_1\right) / f\left(E_2\right)\right)} \tag{2}$$
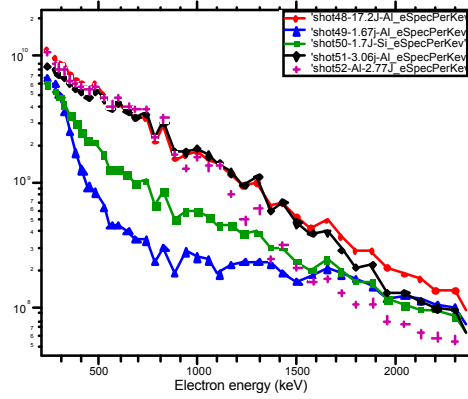
Error!

Figure 2. Electron distributions measured at various laser intensity at Callisto laser. The lowest curve (blue) is for $5x10^{18}$ W/cm^2; The second lowest (green) is for $2x10^{19}$ W/cm^2; The top three are for $6x10^{19}$ W/cm^2 (red cross); $8x10^{19}$ W/cm^2 (black diamonds) and $3x10^{20}$ W/cm^2 (red dots).

Similar observations were made at the RAL Vulcan Nd:glass Petawatt laser. This laser delivers over 400 J of energy onto target in a 400 fs FWHM (full-width at half-maximum) temporal pulse onto a focu spot of about 7-8 μm [4]. The p-polarized laser was incident with at an angle of 28˚ to the target normal. The peak intensity reaches up to $5x10^{20}$ W/cm^2. Our electron spectrometer slit was aligned 15 degrees from the laser beam, i.e. 43 degrees off normal, and 79 cm away from the target. For the same target configuration (Ag target, 50 mm in thickness), we observed drastic changes in the hot electron distribution as a function of laser intensities, as illustrated in Fig. 3. However, at the same intensity, the electron distribution does not vary much for targets made of elements from Al to Ag, a factor of 6 different in nuclear charge Z.
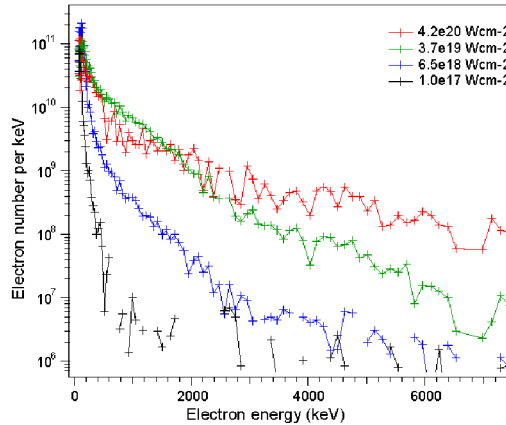

Figure 3. Electron distributions for 50 mm Ag targets at four laser intensities. The hot electron temperatures are 0.1 MeV, 0.4 MeV, 0.7 Mev and 1.6 MeV, respectively, for the four intensities from low to high order.

We plotted the experimental data from both LLNL Callisto and RAL Vulcan laser, in Fig. 4, along side the PIC simulation and ponderomotive scaling. We find that at lower intensities, the experimental data agree with the modeling and theory well, but a discrecpency develops at higher intensities ($>10^{19}$

Wcm^{-2}), with the experimental temperatures being less than the predictions. A fit of the experimental data gives

$$kT_{hot} \sim \left(I\lambda^2\right)^{0.4} \tag{3}$$

Note that this scaling is somewhere between the ponderomotive scaling (Eq.1) and scaling presented by Beg *et. al.* [6], which indicated that $kT_{hot} \sim \left(I\lambda^2\right)^{0.3}$.
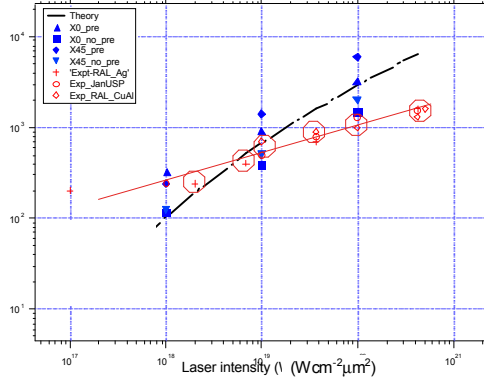

Figure 4. Experimental data (red crosses enclosed in circles) comparing to theoretical scaling (black dashed line) and 2D PIC modeling (as in Figure 1). The red solid line is the fit through the experimental data.

The physics behind this discrepancy between experimental and modeling results could lie in the interaction between short intense laser pulse and solid density plasma. As it has been pointed out earlier [7], for very high laser intensities, the electron density at the interaction surface increases considerably due to self-steepening as the laser pressure far exceeds the material pressure at the critical surface. As the density at this interface increases, the electrons that are generated there are less energetic. This results in lower hot electron temperatures, because the shorter the skin depth of the plasma due to the increase in electron density allows for less penetration of the laser's electron-magnetic field, thus producing less electron acceleration.

3. SUMMARY

We presented experimental measurement of hot electrons at laser intensity up to 5x10^{20} W/cm^2. The fit to the experimental data reveal a scaling of hot electron temperature propotional to 0.4 power of the laser intensity.

References

[1] P. Gibbon and E. Forster, Plasma Phys. Control. Fusion, 38, 769 (1996).
[2] S. C. Wilks, W. L. Kruer, M. Tabak, and A. B. Langdon, Phys. Rev. Lett. 69, 1383 (1992).
[3] H. Chen, P. K. Patel, D. F.Price, B. K. Young, P. T. Springer, R. Berry, R. Booth, C. Bruns, and D. Nelson, Review Scientific Instruments, **74**, 1551, (2003).
[4] P K Patel, M H Key, A J Mackinnon, *et al.* the Fast Ignitor Workshop Proceedings
[5] H. Chen, H. McLean, P. K. Patel, and S. C.Wilks, IFSA 03 (2003).
[6] Beg, F.N., Bell, A. R., Dangoor, A. E., Danson, C. N., Fews, A. P., Glinsky, M. E., Hammel, B. A., Lee, P., Norreys, P. A., and Tatarakis, M. Phys. Plasmas, **4**, 447, (1997)
[7] S. C. Wilks and W. L. Kruer, IEEE J. of Quantum Electronics, **11**, 1954 (1997).